Quantum states without time-reversal symmetry: wavefront dislocations in a non-integrable Aharonov-Bohm billiard

1986 J. Phys. A: Math. Gen. 19 1365

(http://iopscience.iop.org/0305-4470/19/8/018)

J. Phys. A: Math. Gen. 19 (1986) 1365-1372. Printed in Great Britain

Quantum states without time-reversal symmetry: wavefront dislocations in a non-integrable Aharonov–Bohm billiard

M V Berry and M Robnik

H H Wills Physics Laboratory, University of Bristol, Tyndall Avenue, Bristol BS8 1TL, UK

Received 23 August 1985

Abstract. We display complex wavefunctions ψ_j for the jth eigenstate of a particle moving freely in a domain $\mathcal{D}$ (whose reflecting boundary gives classically chaotic motion) threaded by a single line of magnetic flux whose strength (in quantum units) is α. The wavefronts (phase contours of ψ_j) show the expected dislocation singularities both away from the flux line (where their strength is ± 1) and at the flux line (where the strength is the integer closest to α). ψ_5 shows two dislocations away from the flux line for all α, and the birth of a dislocation at the flux line as α passes the value $\frac{1}{2}$. ψ_{50} shows 43 dislocations, in reasonable agreement with a semiclassical theory based on regarding $\psi_{\mathcal{N}}$ as a complex Gaussian random function, which predicts $\mathcal{N}$ dislocations in the asymptotic limit $\mathcal{N} \to \infty$.

1. Introduction

We aim to demonstrate by examples that the complex bound-state wavefunctions for Hamiltonians $\hat{H}$ without time-reversal symmetry do in fact possess the phase singularities that genericity arguments lead us to expect. If the wavefunction ψ is written in terms of modulus ρ and phase χ, namely

$$\psi(\boldsymbol{r}) = \rho(\boldsymbol{r}) \exp(\mathrm{i}\chi(\boldsymbol{r})) \tag{1}$$

then the singularities of χ occur at the zeros of ρ, which generically have codimension two. In the plane the singularities are points; in space they are lines. Nye and Berry (1974) called them wavefront dislocations because of the morphological resemblance between the constant-χ surfaces (wavefronts) and atomic planes near crystal dislocations.

In previous studies (reviewed by Berry 1981), ranging over oceanography, acoustics and optics as well as quantum mechanics, attention was focused on scattering problems (time-dependent as well as stationary). When the geometry of bound states has been considered this has usually been for time-reversible $\hat{H}$ whose wavefunctions are real so that the nodal sets have codimension one—that is, lines in the plane and surfaces in space (see McDonald and Kaufman (1979), Robnik (1984), Berry and Wilkinson (1984) and the discussion in Berry (1983)).

It might be objected that in quantum mechanics it is unrealistic to study phase geometry because $\chi(\boldsymbol{r})$ can be altered by a gauge transformation: replacing the momentum $\boldsymbol{p}$ by $\boldsymbol{p} - \nabla F(\boldsymbol{r})$, where F is any single-valued function, causes χ to change to $\chi + F/\hbar$ without affecting the physical content of the wavefunction. But although such a transformation moves the wavefronts it leaves invariant the dislocations which are precisely the singularities we will study.

0305-4470/86/081365+08$02.50

$\chi(\boldsymbol{r})$ is a single-valued function of position under continuation not involving circuits enclosing dislocations, but changes by $2S\pi$, where S is an integer, around a circuit which does enclose a dislocation. S is the *strength* of the dislocation; generically, $S = \pm 1$.

We will study point dislocations in the bound states of a charged particle moving freely in a planar (billiard) domain $\mathcal{D}$, on whose reflecting walls $\psi(\boldsymbol{r})$ must vanish, threaded by a single line of magnetic flux which in quantum units has strength α (that is, $\alpha =$ charge $\times$ flux$/h$). This is the 'Aharonov-Bohm quantum billiard' introduced by Berry and Robnik (1986, hereafter referred to as BR); we showed that in position representation with $\boldsymbol{r} = (x, y) = (r, \theta)$ and the origin at the flux line, the Hamiltonian is

$$\hat{H} = -[\nabla - \mathrm{i}\alpha \boldsymbol{A}(\boldsymbol{r})]^2 \tag{2}$$

where $\boldsymbol{A}$ is any vector potential describing the localised magnetic field. Thus $\boldsymbol{A}$ must satisfy

$$\nabla \wedge \boldsymbol{A}(\boldsymbol{r}) = 2\pi\delta(\boldsymbol{r}) \qquad \text{i.e.} \oint \boldsymbol{A}(\boldsymbol{r}) \cdot \mathrm{d}\boldsymbol{r} = 2\pi \tag{3}$$

for any positive circuit enclosing the flux line once.

With (2) the wavefunctions ψ_j and energy levels E_j defined by $\hat{H}\psi_j = E_j\psi_j$ possess the symmetries

$$\begin{aligned} E_j(-\alpha) &= E_j(\alpha) & \psi_j(\boldsymbol{r}; -\alpha) &= \psi_j^*(\boldsymbol{r}; \alpha) \\ E_j(\alpha + 1) &= E_j(\alpha) & \psi_j(\boldsymbol{r}; \alpha + 1) &= \mathrm{e}^{\mathrm{i}\theta}\psi_j(\boldsymbol{r}; \alpha). \end{aligned} \tag{4}$$

Therefore all essential structure, including the generic phase singularities in ψ_j, is contained in the flux range $0 \leqslant \alpha \leqslant \frac{1}{2}$, and most of our study will be restricted to this range.

But the physical singularity at $\boldsymbol{r} = 0$ can produce a phase singularity there which is not the same inside and outside the range $0 \leqslant \alpha \leqslant \frac{1}{2}$. Indeed from (4) it follows that changing α by an integer N gives a phase factor $\exp(\mathrm{i}N\theta)$ and so changes the strength S_0 of the dislocation at $\boldsymbol{r} = 0$ by N. However, S_0 is always an integer and so must change discontinuously as α varies smoothly. The jumps in S_0 occur as α passes *half-integer* values. This can also be seen from (4) which implies

$$\psi_j(\boldsymbol{r}; \tfrac{1}{2} + \varepsilon) = \mathrm{e}^{\mathrm{i}\theta}\psi_j^*(\boldsymbol{r}; \tfrac{1}{2} - \varepsilon). \tag{5}$$

This phenomenon also occurs in the Aharonov-Bohm *scattering* wavefunction, where it was studied analytically and experimentally by Berry *et al* (1980); they showed that S_0 is simply *the integer closest to* α and that its jump is associated with a *nodal line* connecting the flux line with infinity. In the present context we expect for half-integer α a nodal line connecting the flux line with the boundary of $\mathcal{D}$. This is associated with the special form of ψ:

$$\psi(\boldsymbol{r}) = f(\boldsymbol{r}) \exp\left(\frac{\mathrm{i}}{2}\int_{\boldsymbol{r}_0}^{\boldsymbol{r}} \boldsymbol{A} \cdot \mathrm{d}\boldsymbol{r}\right) \qquad \text{when } \alpha = \tfrac{1}{2} \tag{6}$$

where f is a *real function* (see BR) which under continuation around the origin changes sign across the nodal line.

In § 2 we study the wavefunction geometry for a low state (ψ_5) as a function of α, including the transition through $\alpha = \frac{1}{2}$ where the first dislocation appears at the flux line. In § 3 we study a high state (ψ_{50}) for a particular value of α and interpret the

distribution of dislocations in terms of a theory in which ψ is regarded as a Gaussian random function of position.

All computations will be for the domain $\mathcal{D}$ whose boundary is given parametrically by

$$\begin{aligned} x &= \cos\phi + B\cos 2\phi + C\cos(3\phi + \mu) \\ y &= \sin\phi + B\sin 2\phi + C\sin(3\phi + \mu) \end{aligned} \tag{7}$$

with $B = C = 0.2$, $\mu = \pi/3$. This is the 'Africa' shape shown in all our figures. It was chosen for three reasons. First, $\mathcal{D}$ is a cubic conformal image of the unit disc, for which our method of solving Schrödinger's equation (fully explained in BR) can be applied. Second, $\mathcal{D}$ has no geometric symmetry and so the genericity of ψ is not threatened by the antiunitary invariance phenomena discussed by Robnik and Berry (1986). Third, the boundary of $\mathcal{D}$ gives rise to classical (bouncing) motion that is certainly non-integrable and indeed completely irregular (according to all our computational evidence) and so the wavefunctions (especially the high-lying ones) ought to display the effects of what has come to be called 'quantum chaos'.

2. Geometry of a low-lying state for different flux values

Without flux ($\alpha = 0$), ψ_j are the real eigenfunctions of the Laplace operator satisfying Dirichlet boundary conditions on the boundary (7). Figure 1 shows the nodal lines and contours of the modulus $\rho_j(r)$ for $j = 5$. There are three nodal cells bounded by nodal lines that meet the boundary perpendicularly, as they must.

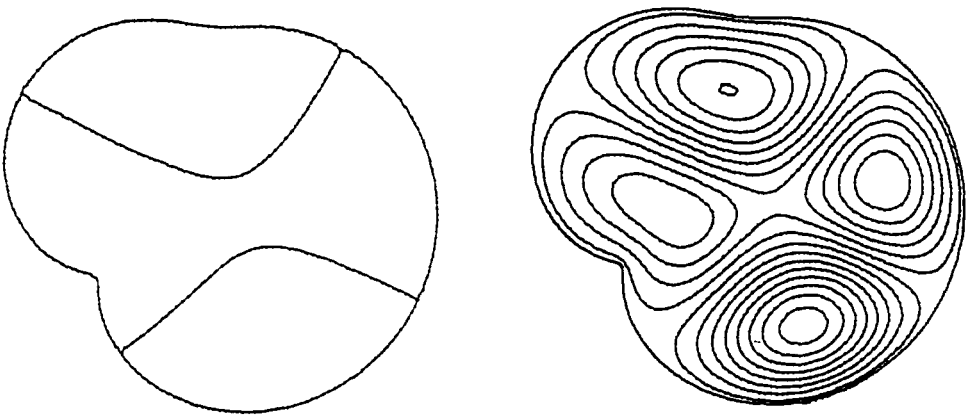

Figure 1. Nodal lines (left) and contours of modulus (right) for the real wavefunction $\psi_5(r)$ in the billiard (7) without flux.

Figure 2 shows ψ_5 for six non-zero values of α. For each α we display the wavefronts (contours of χ at intervals of $\pi/4$), the nodal lines of $\mathrm{Re}\,\psi = \rho\cos\chi$, and the contours of the modulus ρ. (Strictly the nodal pictures are redundant because the information they contain is present in the wavefront pictures (the zero set of $\mathrm{Re}\,\psi$ is the union of the wavefronts $\chi = \pi/2$ and $\chi = 3\pi/2$), but we include them for clarity of presentation.)

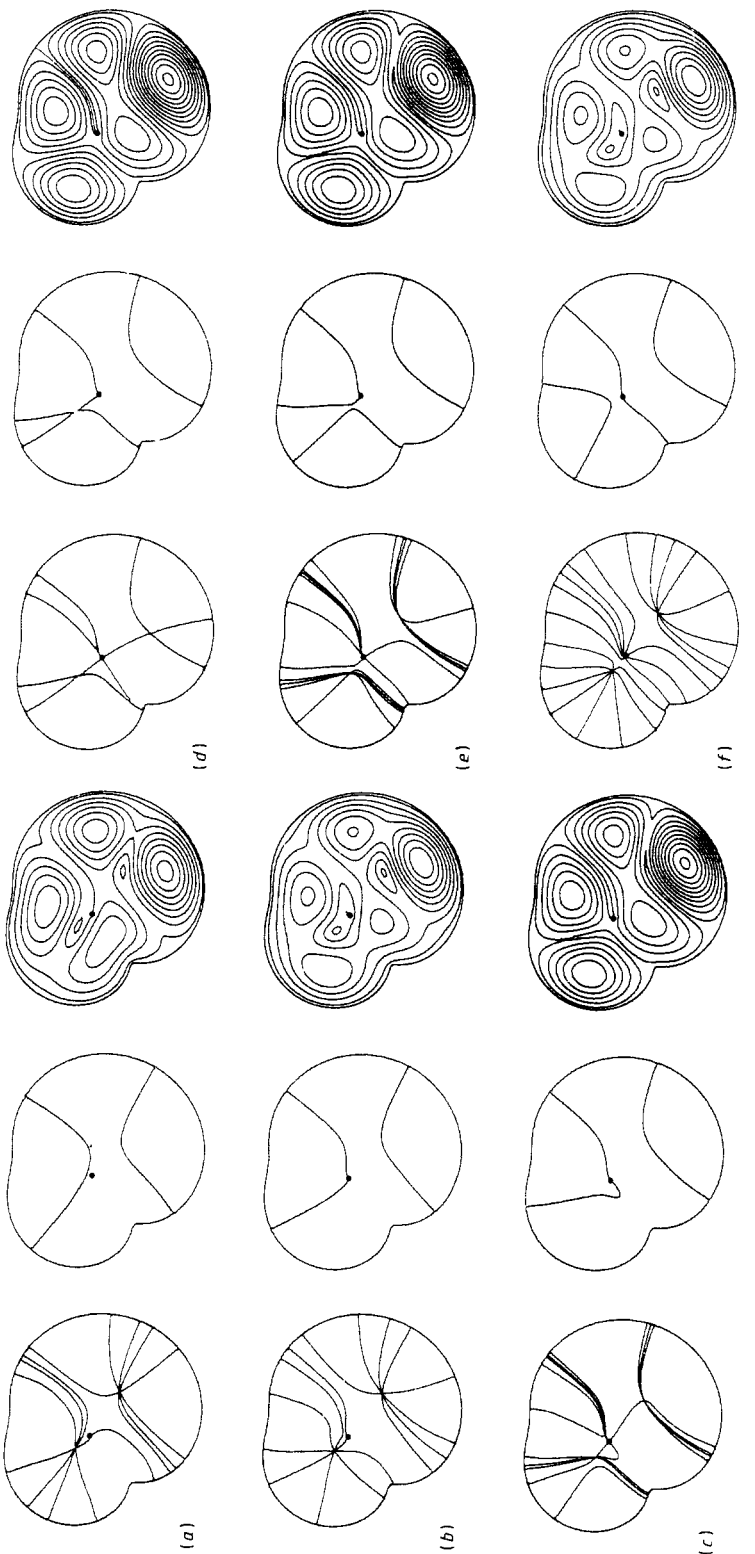

Figure 2. Wavefronts (left), nodal lines of real part (centre) and contours of modulus (right) for the complex wavefunction $\psi_5(\boldsymbol{r})$ in the billiard (7) with flux values (*a*) $\alpha = 0.1$, (*b*) $\alpha = \frac{1}{2}(3-\sqrt{5})$ (1-golden flux); (*c*) $\alpha = 0.49$; (*d*) $\alpha = 0.5$; (*e*) $\alpha = 0.51$; (*f*) $\alpha = \frac{1}{2}(\sqrt{5}-1)$ (golden flux). A dot marks the position of the flux line in each picture.

The most striking features are the two dislocation points, which spring into being as soon as the flux is switched on; their positions hardly change over the whole range $0<\alpha<0.5$. Both dislocations have the same sign: $S=+1$ (for positive circuits). For small flux (e.g. $\alpha=0.1$) the wavefronts are crowded near the nodes of the real wavefunction for zero flux (figure 1).

As α approaches 0.5 (e.g. $\alpha=0.49$) wavefronts crowd near the origin, anticipating the dislocation that will form there. When $\alpha=0.5$ there is the expected nodal line, clearly visible on the modulus picture, connecting the flux line to the boundary. When α just exceeds 0.5 (e.g. $\alpha=0.51$) the dislocation has evidently been formed (with $S_0=+1$) but wavefronts approach it very anisotropically; note that the topology of connection of wavefronts with the other two dislocation points has altered. With further increase of α (e.g. to the golden flux $\alpha=\frac{1}{2}(\sqrt{5}-1)=0.618$), wavefronts distribute themselves more uniformly around this dislocation which now closely resembles the other two; nothing betrays the fact that this one, unlike those, owes its existence to the physical singularity at the flux line. Comparing the golden flux with the 'dual golden' flux $\alpha=1-\frac{1}{2}(\sqrt{5}-1)=0.382$ we see that the modulus pictures are identical, as (5) implies, but the wavefronts (and thus the nodal lines) are not the same, because (5) implies

$$\chi(\boldsymbol{r};\tfrac{1}{2}+\varepsilon)=-\chi(\boldsymbol{r};\tfrac{1}{2}-\varepsilon)+\theta. \tag{8}$$

One obvious feature of figure 2 is the fact that all wavefronts meet the boundary perpendicularly. This is an artefact of our choice of gauge (see BR), in which the lines of $\boldsymbol{A}$ near the boundary are parallel to it ($\boldsymbol{A}$ is the velocity field of a steady irrotational incompressible flow in $\mathcal{D}$, with a point vortex of strength 2π at the origin). With this gauge it follows from the Schrödinger equation that $\nabla^2\psi=0$ on the boundary so that the zero set of any 'projection' $\mathrm{Re}\,\mathrm{i}\psi\exp(-\mathrm{i}\chi_0)$ (i.e. the wavefront with phase $\chi=\chi_0$) must meet the boundary perpendicularly. With a different choice of gauge the wavefronts could be made to meet the boundary at any angle. (Another trivial consequence of gauge freedom is that multiplication by a constant phase factor $\exp(\mathrm{i}\chi_0)$ leaves the pattern of wavefronts unchanged but adds χ_0 to the value of the phase at each point; therefore it would be meaningless to label the phase contours in our pictures, and we have not done so.)

3. The geometry of a high-lying state and its semiclassical interpretation

Figure 3 shows the 50th state for the golden flux $\alpha=\frac{1}{2}(\sqrt{5}-1)$. The most obvious feature of the wavefronts is the proliferation of dislocations, more or less uniformly

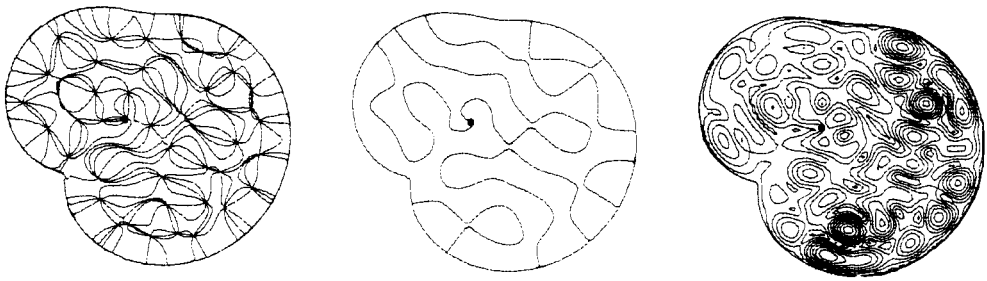

Figure 3. As figure 2 for ψ_{50} and $\alpha=\frac{1}{2}(\sqrt{5}-1)$.

distributed across $\mathscr{D}$ except for a tendency to avoid the boundary: there are 44 of them. The nodal lines of Re ψ_{50} wander without apparent regularity, and have more or less uniform spacing except near avoided crossings (the same morphology was noted by McDonald and Kaufman (1979) in the real wavefunctions of a chaotic billiard without flux). The contours of ρ_{50} show a series of maxima, more or less uniformly distributed and with a tendency to be higher in the bottom right part of $\mathscr{D}$ ('south east Africa'). ψ_{50} is not a low-lying state and so it is natural to seek to understand it in terms of the limited semiclassical theory which is available for such classically non-integrable systems.

This theory (Berry 1977, Voros 1979) (reviewed by Berry 1983) is based on the idea that $\psi(\boldsymbol{r})$ near $\boldsymbol{r}$ is a superposition of waves with wavevectors $\boldsymbol{k}$, related to the momenta $\boldsymbol{p}$ of classical motion near $\boldsymbol{r}$ by de Broglie's relation $\boldsymbol{k}=\boldsymbol{p}/h$ (in this paper we take $\hbar=1$—cf (2)). For a classically ergodic system, such as we assume the Africa billiard to be on the basis of numerical computations of the bounce map, these momenta are uniformly distributed over the energy surface $H(\boldsymbol{r},\boldsymbol{p})=E$. For the Hamiltonian (2) and energy $E\equiv k^2$ this gives wavevectors

$$\boldsymbol{k}_l(\boldsymbol{r})=k\boldsymbol{u}_l+\alpha\boldsymbol{A}(\boldsymbol{r}) \tag{9}$$

where $\boldsymbol{u}_l$ are unit vectors uniformly distributed in direction. This corresponds to the fact that in an ergodic billiard (with or without flux) particles eventually pass almost every point with constant speed but with almost every direction of velocity, and velocity is $\boldsymbol{p}-\alpha\boldsymbol{A}(\boldsymbol{r})$.

In the superposition, the different wavevectors $\boldsymbol{k}_l$ contribute to $\psi(\boldsymbol{r})$ with the same strength but with phases δ_l that can be assumed random (because of the long times separating returns to the neighbourhood of $\boldsymbol{r}$). The model wavefunctions describing quantum states with energies near E are thus members of a *Gaussian random ensemble* with wavevectors (9). The functions in this ensemble can be written

$$\psi_G(\boldsymbol{r};\alpha)=\frac{1}{\sqrt{\mathscr{A}l_{\max}}}\exp\left(\mathrm{i}S_0(\alpha)\int_{r_0}^{r}\mathrm{d}\boldsymbol{r}\cdot\boldsymbol{A}(\boldsymbol{r})\right)\sum_{l=1}^{l_{\max}}\exp(\mathrm{i}k\boldsymbol{u}_l\cdot\boldsymbol{r}+\delta_l) \tag{10}$$

where $\mathscr{A}$ is the area of $\mathscr{D}$, included to ensure that the ψ_G are normalised on the average, and the first exponential factor contains the effects of the vector potential with α replaced by its nearest integer $S_0(\alpha)$ in order to keep ψ_G single-valued, and $l_{\max}\to\infty$. Of course these functions do not satisfy the condition of vanishing on the billiard boundary.

First we discuss the effects of the flux factor. If α is of the order of unity (e.g. the golden flux), its effects are semiclassically negligible (k is large) except for a small region near the flux line whose linear dimensions are comparable with the flux-free wavelength $2\pi/k$ (this is the region within which $S_0(\alpha)|\boldsymbol{A}(\boldsymbol{r})|>kr$). For very large α the phase ψ_G is dominated by the first factor in (10) which simply describes the dislocation at $\boldsymbol{r}=0$, already discussed in § 1.

Figure 4 shows a function ψ_G chosen from the ensemble (10) with $S_0=0$ and k chosen to correspond semiclassically with the energy E_{50}, i.e. $k=(4\pi\times 50/\mathscr{A})^{1/2}$, where $\mathscr{A}$ is the area of $\mathscr{D}$. Qualitatively there is a close resemblance with figure 3, apart from the following three differences. First, there is no tendency for dislocations of ψ_G to avoid the boundary as those of the exact waves ψ_G do. This tendency is of course gauge-independent but in the gauge we are using it arises from the fact that all wavefronts must meet the boundary perpendicularly and so are less likely to intersect close to it. Second, and with the same explanation, there is no tendency for the nodal

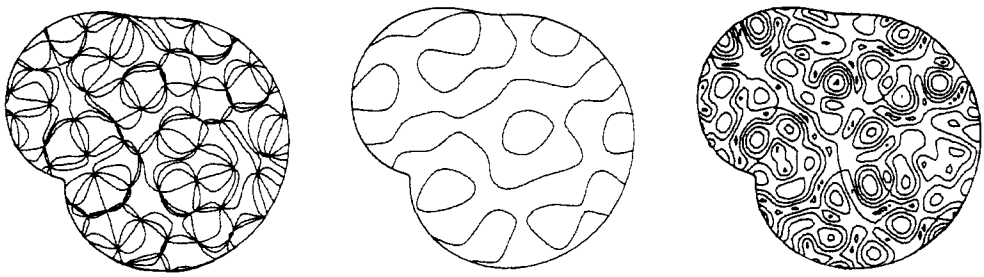

Figure 4. As figure 3 for a simulated wavefunction of the type (10) with k^2 chosen to approximate E_{50}, $l_{\max} = 10$ and δ_l chosen randomly in the range $0 \leq \delta_l \leq 2\pi$.

lines of Re ψ_G to meet the boundary perpendicularly as those of ψ_G do. Third, there is no tendency for the heights of the maxima of ψ_G to be greater near 'south east Africa', as those of ψ_{50} are; we have no explanation for this (it might be a fluctuation, or it might indicate some hidden regularity in the classical motion).

A quantitative prediction of the Gaussian random model (10) is that the expected number of dislocations in the wavefunction $\psi_{\mathcal{N}}$ as $\mathcal{N} \to \infty$ (i.e. semiclassically) is simply $\mathcal{N}$ itself. To derive this result we write (10) as

$$\psi_G(\boldsymbol{r}) \equiv u(\boldsymbol{r}) + \mathrm{i}v(\boldsymbol{r}) \tag{11}$$

and neglect the flux factor which is semiclassically unimportant except when very close to the origin. Dislocations are joint zeros of u and v, so that the number in any area $\mathcal{S}$ is

$$\int\int_{\mathcal{S}} \mathrm{d}\boldsymbol{r}\, \delta(u)\, \delta(v) \det \left| \frac{\partial(u, v)}{\partial(x, y)} \right|. \tag{12}$$

The expectation value of the dislocation density is therefore

$$n = \left\langle \delta(u)\delta(v) \left| \frac{\partial u}{\partial x}\frac{\partial v}{\partial x} - \frac{\partial u}{\partial y}\frac{\partial v}{\partial y} \right| \right\rangle \tag{13}$$

where $\langle\ \rangle$ denotes averaging over the ensemble (10) with random phases δ_l.

It follows from (10) that, at any point, u, v, $\partial u/\partial x \ldots \partial v/\partial y$ are independent Gauss-distributed variables with variances

$$\begin{aligned} &\langle u^2 \rangle = \langle v^2 \rangle = 1/2\mathscr{A} \\ &\left\langle \left(\frac{\partial u}{\partial x} \right)^2 \right\rangle = \ldots \left\langle \left(\frac{\partial v}{\partial y} \right)^2 \right\rangle = \tfrac{1}{4}k^2\mathscr{A}. \end{aligned} \tag{14}$$

In an obvious notation the average (13) is thus

$$\begin{aligned} n &= \langle \delta(u) \rangle^2 \langle |u_x v_x - u_y v_y| \rangle \\ &= \frac{\mathscr{A}}{\pi} \left(\frac{2\mathscr{A}}{\pi k^2} \right)^2 \int_{-\infty}^{\infty}\int_{-\infty}^{\infty}\int_{-\infty}^{\infty}\int_{-\infty}^{\infty} \mathrm{d}u_x\, \mathrm{d}u_y\, \mathrm{d}v_x\, \mathrm{d}v_y |u_x v_x - u_y v_y| \\ &\quad \times \exp\left(-\frac{2\mathscr{A}}{k^2}(u_x^2 + u_y^2 + v_x^2 + v_y^2) \right). \end{aligned} \tag{15}$$

The quadruple integral may be evaluated by introducing polar coordinates in the $u_x u_y$

and $v_x v_y$ planes, with the result

$$n = k^2/4\pi. \tag{16}$$

When applied to the whole domain $\mathscr{D}$ this predicts $\mathscr{A}k^2/4\pi$ dislocations, which is simply the leading (Weyl) term in the asymptotic expansion for the number of levels below k, i.e. $\mathcal{N}$. Therefore we have obtained the result we claimed: the $\mathcal{N}$th state has, on the average, $\mathcal{N}$ dislocations. This conclusion survives a rough attempt to include the tendency of dislocations to avoid the boundary: if we apply (16) not to the whole of $\mathscr{D}$ but to a domain excluding a narrow strip of width k^{-1} (i.e. wavelength/2π) round the boundary, which has length $\mathscr{L}$, the expected number of dislocations becomes

$$(\mathscr{A} - \mathscr{L}/k)k^2/4\pi = \mathscr{A}k^2/4\pi - \mathscr{L}k/4\pi \tag{17}$$

which is precisely the corrected Weyl formula for $\mathcal{N}$.

The number of dislocations in $\psi_{\mathcal{N}}$ is not expected to be exactly $\mathcal{N}$ but to fluctuate from state to state. It seems difficult to estimate the magnitude of these fluctuations, but assuming they are, at least approximately, Poissonian, i.e. $\sqrt{\mathcal{N}}$, we see that the presence of 43 dislocations (excluding $r = 0$) in ψ_{50} accords reasonably well with the theory. We have also computed ψ_{10} and ψ_{20} for the golden α, and found 8 and 16 dislocations respectively, thus lending further credibility to the theoretical predictions. (Inspection of our pictures suggests that the boundary avoidance zone is somewhat wider than the $1/k$ we have assumed, and more like a quarter of a wavelength; if this is assumed, the predicted dislocation number becomes $\mathcal{N} - 0.588\sqrt{\mathcal{N}}$ which for $\mathcal{N} = 50$, 20 and 10 gives 46, 17 and 8 dislocations—much closer to the observed numbers.)

Acknowledgments

We thank Dr F J Wright for a helpful suggestion. This research was not supported by any military agency. MR was supported by a grant from the UK Science and Engineering Research Council.

References

Berry M V 1977 *J. Phys. A: Math. Gen.* **10** 2083-91

—— 1981 *Physics of Defects* (*Les Houches Lectures XXXIV*) ed R Balian, M Kleman and J Poirier (Amsterdam: North-Holland) pp 453-543

—— 1983 *Chaotic Behaviour of Deterministic Systems* (*Les Houches Lectures XXXVI*) ed G Iooss, R H L G Helleman and R Stora (Amsterdam: North-Holland) pp 171-271

Berry M V, Chambers R G, Large M D, Upstill C and Walmsley J C 1980 *Eur. J. Phys.* **1** 154-62

Berry M V and Robnik M 1986 *J. Phys. A: Math. Gen.* **19** 649-68

Berry M V and Wilkinson M 1984 *Proc. R. Soc.* A **392** 15-43

McDonald S W and Kaufman A N 1979 *Phys. Rev. Lett.* **42** 1189-91

Nye J F and Berry M V 1974 *Proc. R. Soc.* A **336** 165-90

Robnik M 1984 *J. Phys. A: Math. Gen.* **17** 1049-74

Robnik M and Berry M V 1986 *J. Phys. A: Math. Gen.* **19** 669-82

Voros A 1979 *Stochastic Behaviour in Classical and Quantum Hamiltonian Systems* (*Lecture Notes in Physics* **93**) ed G Casati and J Ford (Berlin: Springer) pp 326-33